

## Research Article

# Isoxyl Aerosols for Tuberculosis Treatment: Preparation and Characterization of Particles

Chenchen Wang<sup>1</sup> and Anthony J. Hickey<sup>1,2</sup>

Received 23 November 2009; accepted 2 March 2010; published online 26 March 2010

**Abstract.** Isoxyl is a potent antituberculosis drug effective in treating various multidrug-resistant strains in the absence of known side effects. Isoxyl has been used exclusively, but infrequently, via the oral route and has exhibited very poor and highly variable bioavailability due to its sparing solubility in water. These properties resulted in failure of some clinical trials and, consequently, isoxyl's use has been limited. Delivery of isoxyl to the lungs, a major site of *Mycobacterium tuberculosis* infection, is an attractive alternative route of administration that may rescue this abandoned drug for a disease that urgently requires new therapies. Particles for pulmonary delivery were prepared by antisolvent precipitation. Nanofibers with a width of 200 nm were obtained by injecting isoxyl solution in ethanol to water at a volume ratio of solvent to antisolvent of 1:5. Based on this preliminary result, a well-controlled method, involving nozzle mixing, was employed to prepare isoxyl particles. All the particles were 200 to 400 nm in width but had different lengths depending on properties of the solvents. However, generating these nanoparticles by simultaneous spray drying produced isoxyl microparticles (Feret's diameter, 1.19–1.77  $\mu\text{m}$ ) with no discernible nanoparticle substructure. The bulking agent, mannitol, helped to prevent these nanoparticles from agglomeration during process and resulted in nanoparticle aggregates in micron-sized superstructures. Future studies will focus on understanding difference of these isoxyl microparticles and nanoparticles/nanoparticle aggregates in terms of *in vivo* disposition and efficacy.

**KEY WORDS:** antisolvent precipitation; multidrug resistant; pulmonary delivery; spray drying; tuberculosis.

## INTRODUCTION

Tuberculosis is the leading cause of death by a single infectious microorganism. One third of the world's population has been infected by tuberculosis, with 9.27 million new cases and 1.8 million deaths in 2007 according to World Health Organization report 2009 (1). The availability of the vaccine Bacillus Calmette–Guerin and curative chemotherapies were responsible for the general decrease in tuberculosis mortality in the past century. Nevertheless, the frequency of occurrence of new cases began to increase in the mid-1980s. Two main factors contribute to the resurgence of tuberculosis, the occurrence of immunosuppressive diseases, human immunodeficiency virus infections, and the emergence of multidrug-resistant (MDR) strains, which are resistant to isoniazid and rifampicin, two first-line antituberculosis drugs (2–5).

Pulmonary tuberculosis is a major manifestation of tuberculosis implicated in morbidity and systemic dissemination. However, when antitubercular drugs are administered orally, drug concentrations in plasma and the lungs are well

below the suggested therapeutic range in some patients (6–8). Additionally, the fraction of an oral dose of drug delivered to the lungs that can access granulomas, tubercles, or lesions which have very poor blood supply may be small (9). This suboptimal drug concentration contributes to prolonged duration of treatment, relapse, and development of MDR strains. In comparison, inhalation of drugs can avoid this malabsorption in the following ways: (1) Drugs can achieve higher lung tissue to plasma concentration ratio (10); (2) hydrophobic drugs have higher solubility and more rapid dissolution rates in the surface lining fluid containing large quantities of lung surfactants (11); (3) the lungs are thought to have fewer metabolizing enzymes and efflux transporters in contrast to the gastrointestinal tract where orally administered drugs undergo first-pass effects of the gut and liver (12); and (4) more importantly, drug particles delivered to the lungs have been shown to target to macrophages/monocytes, the host cells for *Mycobacterium tuberculosis* (MTB) (13).

Isoxyl (ISO, thiocarlide, 4,4'-diisoamylthio-carbanilide) is a second-line drug used clinically to treat tuberculosis in the 1960s. It is a potentially efficient antituberculosis drug for treatment of the MDR strains in monotherapy or in a combined regimen. *In vitro* studies showed that isoxyl have strong antimycobacterial activity with minimum inhibitory concentration (MIC) of 2.5  $\mu\text{g}/\text{ml}$  for MTB H37Rv and MIC of 1–10  $\mu\text{g}/\text{ml}$  for various clinical isolates of strains resistant to rifampicin and isoniazid (14). However, the effectiveness of

<sup>1</sup> Eshelman School of Pharmacy, Division of Molecular Pharmaceutics, University of North Carolina at Chapel Hill, Campus Box #7571, 1310 Kerr Hall, Chapel Hill, North Carolina 27599, USA.

<sup>2</sup> To whom correspondence should be addressed. (e-mail: ahickey@unc.edu)

isoxyl has been questioned due to failure in some clinical trials (15,16). The most plausible explanation for these failures is that isoxyl is almost completely insoluble in water (solubility calculated by advanced chemistry development (ACD/labs) software V8.14 for Solaris:  $1.3 \times 10^{-6}$  mol/L at 25°C) and, consequently, exhibits poor dissolution and bioavailability when it is delivered exclusively by the oral route. Efforts to improve the oral absorption of isoxyl, including use of micropowders or suspension in olive oil, *etc.*, resulted in no improvement of isoxyl absorption, and the majority of the administered dose was still eliminated intact via the feces (17,18). Pulmonary delivery of isoxyl may be an effective approach to rescue this abandoned drug.

Particle size distribution impacts on drug deposition and disposition. Microparticles with aerodynamic diameter between 1 and 5  $\mu\text{m}$  are delivered from dry powder inhalers to the lungs (19,20) where they are efficiently phagocytized by alveolar macrophages (13,21,22). Targeting to alveolar macrophages is known to enhance efficacy due to specific drug action at the main site of infection (23) and through macrophage activation (24). In contrast to microparticles, nanosuspension can be given by nebulization. It was reported that particles smaller than 500 nm in diameter were phagocytized by alveolar macrophages to a smaller extent than 1–5  $\mu\text{m}$  microparticles (13,22,25). Dendritic cells may take up these nanoparticles (9), but the kinetics of this phenomenon will be influenced by rapid dissolution of the particles in alveolar lining fluid. Consequently, a portion of nanoparticles may escape from monocyte uptake, which leads to an increase in systemic drug exposure. A balance between phagocytosis and dissolution would be beneficial for tuberculosis therapy. Tuberculosis is a systemic infection, which might benefit from higher concentrations of isoxyl in the lungs while requiring maintenance of therapeutically effective plasma concentrations.

This paper describes optimization of antisolvent precipitation conditions with or without simultaneous spray drying to produce isoxyl particles with diverse particle size distributions and morphology suitable for lung delivery. Antisolvent precipitation is a simple method, by which the crystallinity of drugs can be controlled and high drug loadings can be achieved. Precipitation of particles can be induced by introducing a large quantity of antisolvent to drug solution, which results in effectively instantaneous lowering of solvent capacity to solubilize drug (26). The mechanism of precipitation includes three processes: nucleation, coagulation, and condensation. Addition of antisolvent to the drug solution creates high degree of local supersaturation, which leads to the formation of many small nuclei (27,28). These nuclei then undergo growth by condensation and coagulation until reaching an equilibrium (26). Therefore, the solid-state properties including particle size distribution and morphology of the resulting precipitants can be influenced by the factors that have impact on the rates of these three processes (26,29). Spray drying generated dry powders from particle suspension following antisolvent precipitation. In the spray-drying process, particle size and shape can also be changed by varying feed properties, atomization conditions, and drying process (30).

## MATERIALS AND METHODS

### Materials

Isoxyl was purchased from Cayman Chemical Co. (Ann Arbor, MI, USA). Acetone and isopropanol were obtained from Fisher Scientific. D-mannitol and ethanol were from Sigma. Tetrahydrofuran (THF) was from EM Science (Darmstadt, Germany). Lactose (Respitose® ML001) was provided by DMV internal. Flexi-Dry™ freeze-dryer was from Kinetics Group (Santa Clara, CA, USA). The three-fluid nozzle was purchased from Buchi Labortechnik AG (Flawil, Switzerland) and fit in a BUCHI B-191 mini-spray drier made by the same manufacturer. Isopore™ polycarbonate membrane filter (pore size, 0.1  $\mu\text{m}$ ; Millipore, Billerica, MA, USA) or a Cyclopore polycarbonate membrane filter (pore size, 0.1  $\mu\text{m}$ , Whatman, Florham Park, NJ, USA) was used to collect particles in suspensions. Water was deionized by Barnstead Nanopure Infinity Ultrapure Water System (Dubuque, IA, USA). Either scanning electron microscopy (SEM; JSM 6,300 V SEM, JEOL USA, Peabody, NY, USA) or SEM (Hitachi S-4700 cold cathode field emission SEM) was used to visualize the particles. Laser diffraction (LD, Series 2600C Malvern Instruments, Malvern, UK) and dynamic light scattering (Nicom particle sizing systems, Autodilute<sup>PAT</sup> Model 370, Santa Barbara, CA, USA) were utilized to measure microparticle and nanoparticle size distributions, respectively. Thermal properties of isoxyl were measured by differential scanning calorimetry (DSC, Perkin Elmer DSC 6, Waltham, MA, USA).

### Particle Manufacture

1. Particles precipitated from the injection method: The preliminary screening of precipitation conditions was performed by injecting isoxyl (1 mg/ml) solution in ethanol into the aqueous phase manually at a speed of approximate 15 ml min<sup>-1</sup> during magnetic stirring using a 27-gauge sterile needle with a 10-ml disposable syringe. The tip of the needle was located just above the stir bar to achieve maximum mixing. Three volume ratios of solvent to antisolvent (VRSA) were assessed: 1:1, 1:2, and 1:5. All the above procedures were conducted at room temperature. The resulting isoxyl particle suspensions were centrifuged (Beckman Model CS-15R) at 8,000–9,000 rpm for 10 min and then the supernatants were discarded. The pellets were transferred to the freeze-dryer (temperature, <–50°C and pressure, <0.05 mbar) and dried for 24 to 48 h.
2. Particles precipitated from the nozzle-mixing method: Solvent and antisolvent at a VRSA equal to 1:5 were mixed by a three-fluid nozzle. Isoxyl concentrations in ethanol, isopropanol, acetone, and THF were 11, 7, 100, and 100 mg/ml, respectively. This was determined by solubility of isoxyl in these solvents. All the other antisolvent precipitation conditions were kept constant: organic feed rate 0.2 ml/min, water feed rate 1 ml/min, nitrogen flow rate 400 L/min, and atomization pressure 3 bar.

Atomized fine droplets from the 0.7-mm diameter nozzle were sprayed directly into 50 ml quenching water. Dynamic light scattering was used to measure particle size distribution in the suspensions. The particles in suspension were collected by filtering through a membrane filter. The filters were completely dried in a vacuum desiccator and used immediately for SEM.

3. Spray-dried particles from the nozzle-mixing method: The effects of processing parameters on particle characteristics were evaluated utilizing a  $2^{7-4}$  factorial design. Eight manufacturing runs were conducted and randomized by Design Expert® (Table I). For all the studies, the aspirator rate of the spray drier was kept at 90% of maximum flow (approximately  $35 \text{ m}^3 \text{ h}^{-1}$ ). Water and isoxyl solution in either isopropanol or ethanol were delivered to the three-fluid nozzle and then sprayed into a BUCHI B-191 mini-spray drier. The particles impacted on the bottom of cyclone (<8 cm from the bottom edge) and collecting vessel and were collected and subsequently characterized. In addition to alcohol, THF as solvent was also evaluated. Isoxyl was dissolved in THF at a concentration of 100 mg/ml and spray dried using the following condition: organic feed rate 0.5 ml/min, water feed rate 1.8 ml/min, atomization pressure 3 bar, nitrogen flow rate 600 L/min, and aspirator rate 90% of maximum flow.

The use of the bulking agent, mannitol, was assessed. The isoxyl solution (7.2 mg/ml) of 4 ml and water were mixed in the three-fluid nozzle under the following conditions: organic feed rate 0.3 ml/min, water feed rate 1.7 ml/min, nitrogen flow rate 400 L/min, and atomization pressure 3 bar. The mixture was directly sprayed into 200 ml of mannitol solution (0.63 mg/ml). This resulted in the ratio of isoxyl to mannitol equal to 1:4.4. The dried particles were resuspended in water to dissolve mannitol. Particle size distributions were measured by dynamic light scattering. To visualize these particles, the suspension was filtered by a membrane filter. The filter was washed with a large quantity of water at least three times to remove residual mannitol and then dried in a vacuum desiccator to be ready for SEM.

## Characterization

1. Particle size and morphology: The primary particle size, shape, and surface morphology of the isoxyl particles were examined by SEM. The lyophilized particles and commercial isoxyl powders were employed as controls and directly applied to conductive double-sided tapes attached to aluminum stubs. The spray-dried particles are first suspended in water and sonicated for 30 s. Small drops of the particle suspensions were placed on the tape and dried in a vacuum desiccator. The filters containing nanoparticles were cut to fit and placed on the tapes. All the samples were sputter-coated using either a Polaron 5200 (Structure Probe Supplies, West Chester, PA, USA) or a Cressington 108 with a Cressington MTM-10/10A high resolution film thickness monitor (Cressington Scientific Instruments, Cranberry, PA, USA) with gold-palladium alloy, and micrographs of the particles were taken. The primary particle size distributions and circularities were calculated by Image J program (Image Processing and Analysis in Java, created by NIH image for Macintosh). Here, the circularity indicates degree of particle elongation and a value approaching unity means that the particles are nearly spherical.

LD was used to measure microparticle size distribution, by volume. Briefly, the microparticles were suspended in water and sonicated for 1–2 min. The suspensions were added dropwise in a stirred sample cell containing distilled water until an obscuration level of about 10% to 20% were achieved. Nanosuspensions from precipitation or particle in mannitol matrix were redispersed in water, and nanoparticle size distributions were measured by dynamic light scattering.

2. Thermal properties of spray-dried microparticles: Thermal profiles of unprocessed isoxyl powder and a batch of spray-dried isoxyl microparticles (condition 8) were subjected to DSC, in which nitrogen at a flow rate of 30 ml/min was the purge gas. The samples were sealed in standard aluminum pans and heated from 21°C to 250°C at scanning rates of 40°C/min and 5°C/min.

**Table I.** A  $2^{7-4}$  Factorial Design for Isoxyl Particle Preparations

	Organic solvent	Organic feed (ml/min)	Water feed (ml/min)	Isoxyl concentration (mg/ml)	Inlet temperature (°C)	N <sub>2</sub> pressure (bar)	N <sub>2</sub> flow (L/min)
1	Isopropanol	0.3	1.8	2	120	3	600
2	Ethanol	0.3	0.7	5	120	6	600
3	Isopropanol	0.3	0.7	2	100	6	800
4	Ethanol	0.7	1.8	2	100	6	600
5	Ethanol	0.3	1.8	5	100	3	800
6	Ethanol	0.7	0.7	2	120	3	800
7	Isopropanol	0.7	1.8	5	120	6	800
8	Isopropanol	0.7	0.7	5	100	3	600

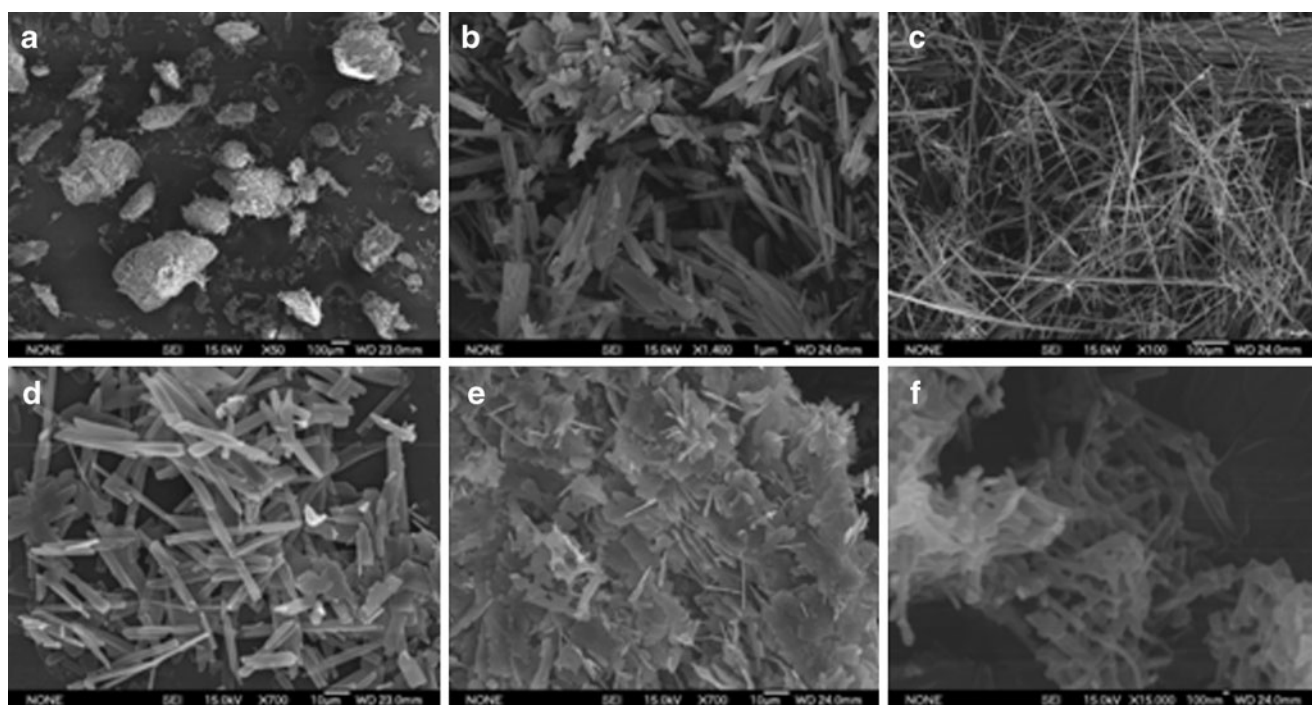


**Fig. 1.** Scanning electron photomicrographs of **a** commercial isoxyl (lot no. 130365–149120) at  $\times 50$  magnification, **b** commercial isoxyl (lot no. 130365–149120) at  $\times 1,400$  magnification, **c** commercial isoxyl (lot no. 165311–167669) at  $\times 100$  magnification, and the isoxyl particles from antisolvent precipitation by injection method: **d** VRSA=1:1 at  $\times 700$  magnification, **e** VRSA=1:2 at  $\times 700$  magnification, and **f** VRSA=1:5 at  $\times 15,000$  magnification

3. Fine particle fraction (FPF) and emitted dose: Aerosolization of the lyophilized isoxyl particles from the injection method, the spray-dried particles (condition 8), and control from commercial source were determined. Lactose carrier was added by mixing isoxyl microparticles at a concentration of 1% *w/w* (Fischer Scientific hematology/chemistry mixer, model 346) for 10 min. Isoxyl powders of approximately 1 mg with or without lactose carrier were filled into the gelatin capsule (product size no. 3; Capsugel, Peapack, NJ, USA) and then placed in an Inhalator® (Boehringer Ingelheim). A twin-stage liquid impinger was employed to evaluate deposition of the isoxyl particles. The impinger (7 and 30 ml of ethanol were placed in the upper and the lower stages) was assembled to be airtight and vertical. After turning on the pump providing airflow of 60 L/min, isoxyl powder was released from the inhalator. The pump was turned off 10 s after emission. After disassembling the apparatus, the capsule shell, the inhaler device, the

mouthpiece, the throat, and the upper and lower stages were all thoroughly washed with ethanol separately. When isoxyl was dissolved in ethanol, the absorption maximum wavelength was 273.5 nm. The concentration of isoxyl in each sample was determined by UV spectrometry at a wavelength of 273.5 nm based on standard curves ( $R > 0.99$ ). Several parameters of the deposition profile of each isoxyl powder were calculated: the emitted dose is the total drug mass leaving the device (the sum of the amount of isoxyl in the mouthpiece, the throat, and the two stages); the recovered dose (RD) includes emitted dose and the amount in the capsule shells and the inhalator device; the fine particle dose (FPD) is the amount of isoxyl in the lower stage, which contains particles ( $\leq 6.4 \mu\text{m}$  aerodynamic diameter); the FPF is the ratio of the FPD to RD; the percent recovery is the ratio of RD to the expected dose; the dispersibility is the ratio of FPD to emitted dose; and the percent emission is the ratio of emitted dose to RD (31).

**Table II.** The Count Median Diameter (CMD) of the Shortest Dimension and the Geometric Standard Deviation (GSD) of the Elongated Isoxyl Particles in Each Powder

		Unprocessed (lot no. 130365–149120)	Unprocessed (lot no. 165311–167669)	VRSA=1:1	VRSA=1:2	VRSA=1:5
Width	CMD ( $\mu\text{m}$ )	1.47	3.95	3.30	0.88	0.22
	GSD	1.88	1.57	1.68	2.03	1.55
Length	CMD ( $\mu\text{m}$ )	8.2	178	17.0	ND	0.99
	GSD	1.90	2.48	1.91	ND	1.66

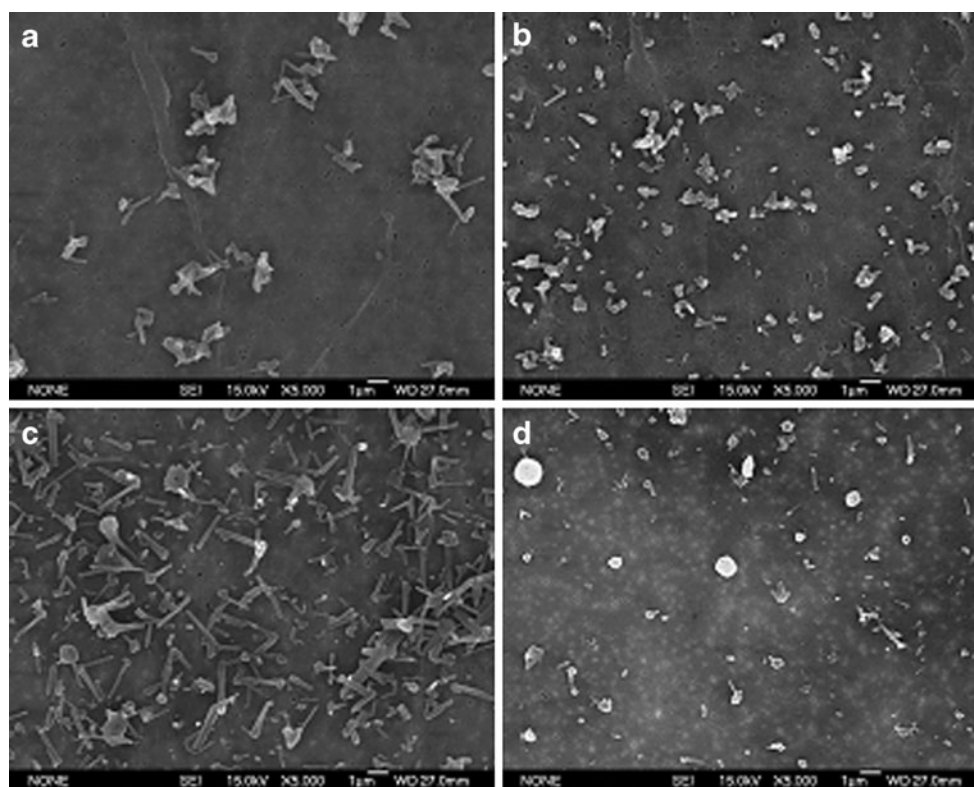


**Fig. 2.** Scanning electron micrographs of isoxyl particles precipitated from ethanol **a**, isopropanol **b**, acetone **c**, and tetrahydrofuran **d**. The micrographs were taken at  $\times 500$  magnification

## RESULTS

### Particle Size Distribution and Morphology

1. Particles precipitated from the injection method: As shown in Fig. 1 and Table II, the commercial isoxyl powder consisted of either large needle-shaped agglomerates (lot no. 130365–149120) or extremely long needle-shaped particles (lot no. 165311–167669) with heterogeneous distributions. Depending on different lots, these particles may form agglomerates with diameters up to a few hundred microns. When isoxyl was precipitated by the injection method from the mixture of VRSA of 1:1, the particles were needle-shaped with count median diameter of 3.3  $\mu\text{m}$  in width and were more loosely aggregated compared to commercial isoxyl. The antisolvent precipitation when VRSA was equal to 1:2 generated both flake-shaped and needle-shaped particles. Changing VRSA to 1:5 yielded elongated particles with shortest dimension of 220 nm (Fig. 1 and Table II).
2. Particles precipitated from the nozzle-mixing method: Depending on organic solvents, isoxyl particle size and morphology were different as shown in Fig. 2 and Table III: ethanol generated nanofibers (width=385 nm, circularity=0.72); isopropanol and THF produced oblate spherical particles (width=275 nm and circularity=0.89 for isopropanol, width=220 nm and circularity=0.87 for THF); and acetone yielded both nanofibers (width=200 nm, circularity=0.4) and oblate spherical nanoparticles (width=

**Table III.** Particle Size Distributions of Isoxyl Particles Precipitated from Various Organic Solvent

		Ethanol	Isopropanol	THF	Acetone	
					Nanofiber	Oblate sphere
Circularity		0.72	0.89	0.87	0.40	0.98
Width	CMW (nm)	385	275	220	200	285
	GSD	1.5	1.47	1.76	1.44	1.3
Length	CML (nm)	1,280	495	450	1,190	390
	GSD	1.72	1.61	1.63	1.66	1.5

*PSD* particle size distribution, *CMW* count median width, *CML* count median length, *GSD* geometric standard deviation

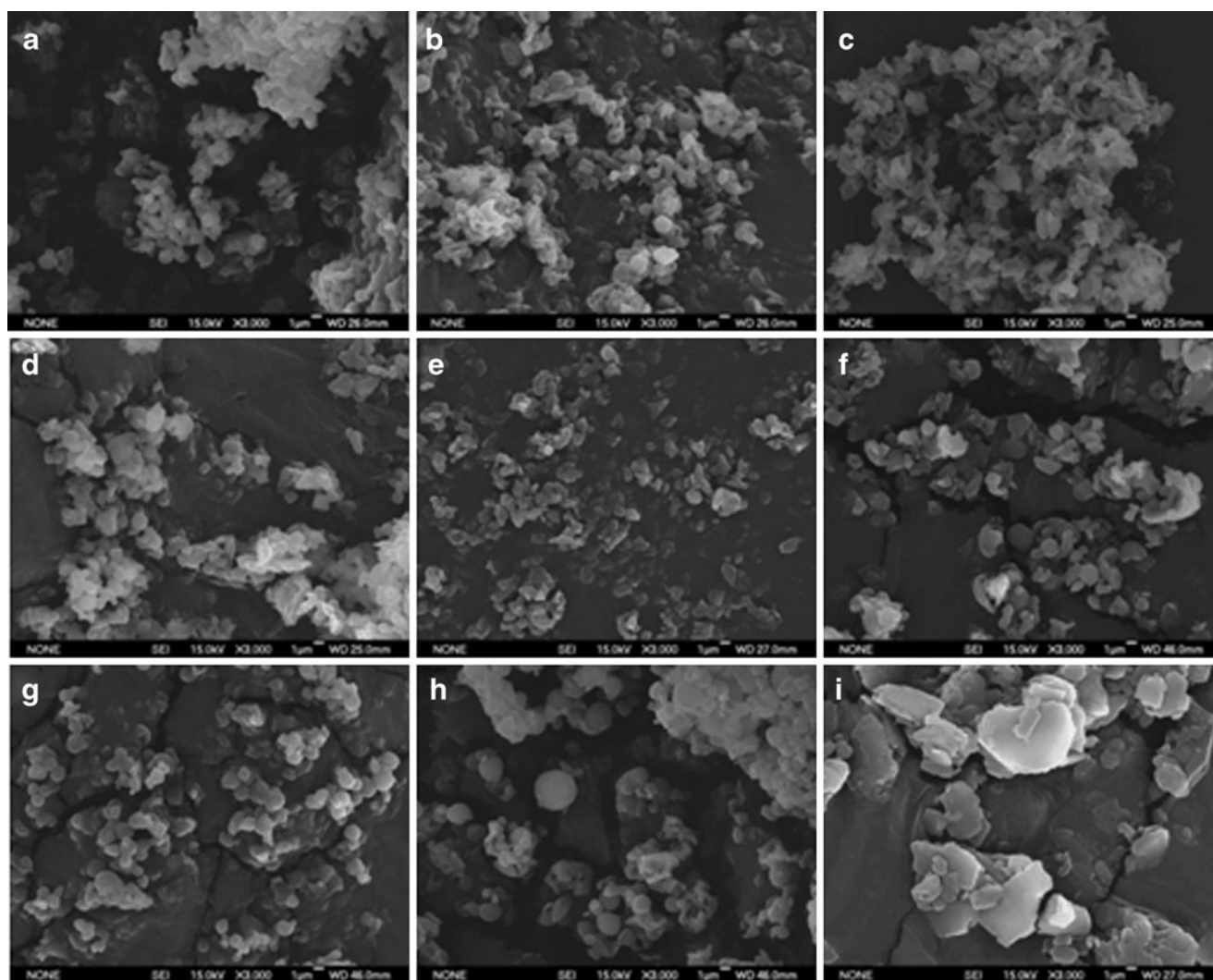


**Fig. 3.** Scanning electron photomicrographs of the spray-dried isoxyl particles produced by nozzle mixing of isoxyl solutions and water. **a–h** The particles from conditions 1–8, respectively, in Table I, and **i** is those from using tetrahydrofuran as solvent. The photomicrographs were taken at  $\times 3,000$  magnification

285 nm, circularity=0.98). Isopropanol was the first choice of solvent for further optimization of nanoparticle preparation because they produced most homogenous nanoparticles with a diameter  $< 500$  nm.

3. Spray-dried particles from the nozzle mixing: The modified spray drier produced approximate spherical particles with count median diameters (Feret's diameter (32)) between 1.19 and 1.77  $\mu\text{m}$  in these eight

**Table IV.** Summary of Particle Size Distributions and Circularities Produced in the Eight Conditions

		1	2	3	4	5	6	7	8
Yield		19.7	29.3	11	25	18.2	11.4	20	28.6
SEM	CMD ( $\mu\text{m}$ )	1.25	1.24	1.82	1.57	1.33	1.19	1.67	1.77
	GSD	2.01	1.58	1.75	1.34	1.21	1.26	1.47	1.48
	Circularity	0.95	0.93	0.91	0.95	0.91	0.95	0.95	0.98
LD	$D_{v,10}$ ( $\mu\text{m}$ )	1.88	1.84	1.98	1.81	1.54	1.86	1.77	1.81
	$D_{v,50}$ ( $\mu\text{m}$ )	2.20	2.16	2.44	2.13	1.81	2.09	2.02	2.14
	$D_{v,90}$ ( $\mu\text{m}$ )	6.43	5.78	7.09	6.05	2.36	2.32	2.28	2.67
	Span	2.06	1.82	2.09	1.98	0.45	0.22	0.26	0.4

PSD particle size distribution, CMD count median diameter, GSD geometric standard deviation, Circularity  $4\pi \cdot (\text{area per square perimeter})$ ,  $D_{v,10}$  particle size at tenth percentile of the cumulative distribution,  $D_{v,50}$  particle size at 50th percentile of the cumulative distribution,  $D_{v,90}$  particle size at 90th percentile of the cumulative distribution, Span  $(D_{v,90} - D_{v,10}) / D_{v,50}$

conditions. The average circularity of the microparticles in each condition was approximate to unity, and those from condition 8 were almost perfect spheres (Fig. 3a–h and Table IV). The particle size distributions, by LD, were unimodal for conditions 5 to 8, bimodal for conditions 2 and 4, and multimodal for conditions 1 and 3. Conditions 5 to 8 resulted in 100% of the particles having diameters  $<5 \mu\text{m}$ ; conditions 1 to 4 resulted in 70–80%  $<5 \mu\text{m}$  (Fig. 4). The yields of the spray-drying conditions varied from 11.0% to 29.3% (Table IV). Statistical experimental design and analysis showed that isoxyl concentration and nitrogen flow rate were two critical factors influencing the yield: an increase in isoxyl concentration and decrease in nitrogen flow rate resulted in greater yield. However, statistical analysis could not identify

any key factors influencing particle size distribution and morphology (Fig. 5). THF was evaluated as a solvent. Unfortunately, this produced much larger plate-shaped particles with heterodisperse particle size distribution (Fig. 3i). Condition 8 appeared to achieve the desired high yield, spherical shape, and narrow particle size distribution.

The addition of mannitol reduced the particle size. When the drug ratio to mannitol is 1:4.4, the mean count diameter of the isoxyl particles determined by DLS was 455 nm, and standard deviation was 299 nm (Fig. 6a). However, SEM micrographs showed that these isoxyl particles were heterogeneous: some particles were almost spherical, while others were elongated (Fig. 6b). Further studies are required to produce nanoparticle aggregates with uniform shape and size.

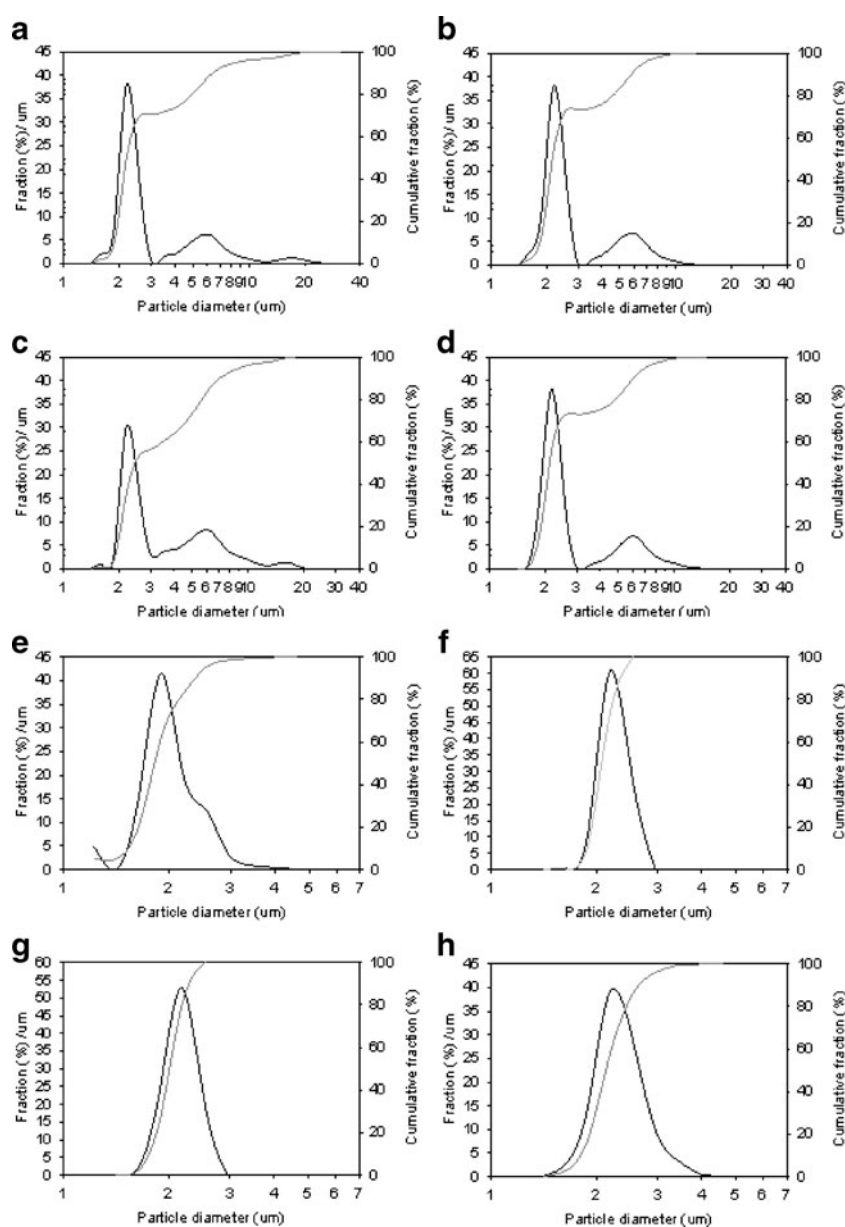


**Fig. 4.** Particle size distributions of the isoxyl particles measured by laser diffraction (LD). a–h represent particles from spray drying condition 1–8

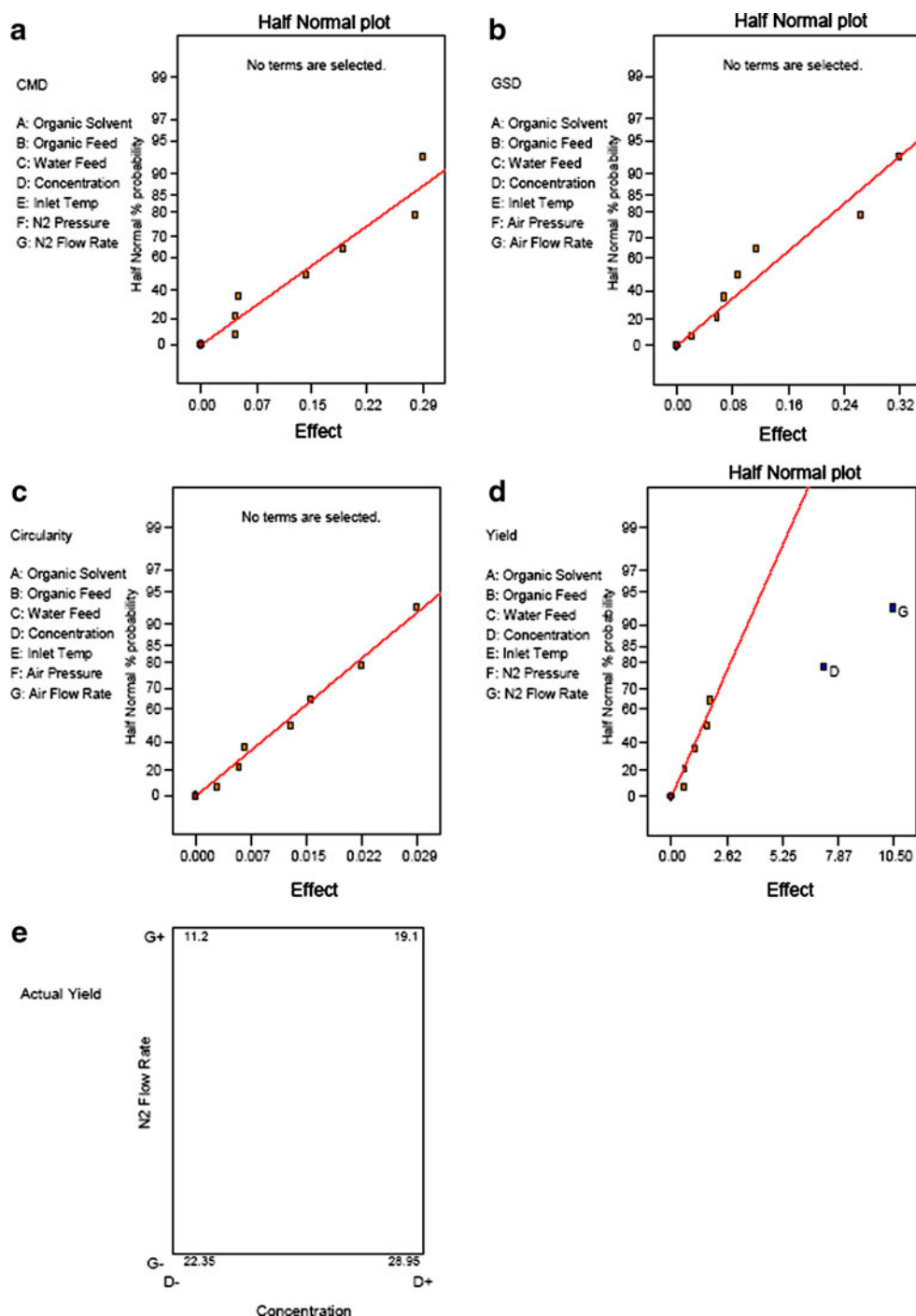


**Fig. 5.** Half normal plot of effects of processing parameters on count median diameter **a**, geometric standard deviation **b**, circularity **c**, and yield **d** of spray-dried isoxyl particles. In the selected range, only yield was influenced by the processing parameters, N<sub>2</sub> flow rate ( $P=0.0025$ ), and isoxyl concentration ( $P=0.0005$ ). **e** Square plot of effect of these two parameters on yield

### Thermal Properties

At a scanning rate of 40°C/min, the DSC thermogram of unprocessed isoxyl powder showed two peaks at 95.8°C and 149.7°C ( $\Delta H=98.6$  J/g), which corresponded to the boiling point of residual ethanol and melting point of isoxyl crystal form I, respectively. Isoxyl microparticles from antisolvent precipitation and consequent spray drying

exhibited only one peak at 143.5°C ( $\Delta H=76.3$  J/g) corresponding to crystal form II (Fig. 7a). This may be explained by the processing conditions removing residual ethanol and converting isoxyl from form I to form II. For the scanning rate of 5°C/min, the DSC thermogram revealed the same results except that the peaks of crystal form I, II, and ethanol shifted to 140.5°C, 136.2°C, and 80.2°C (Fig. 7b).



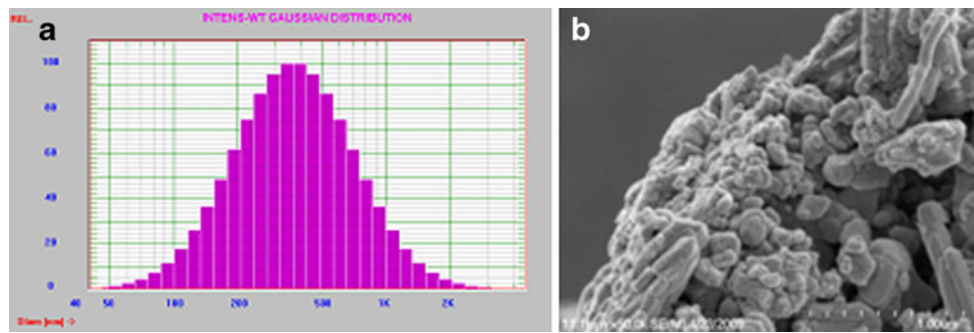


**Fig. 6.** Particle size distribution **a** and scanning electron microscopy **b** of the spray-dried isoxyl particles produced by addition of mannitol (isoxyl:mannitol=1:4.4)

### Fine Particle Fraction and Emitted Dose

1. Particles precipitated from the injection method: The isoxyl particles, which were prepared by injecting isoxyl solution into water and sequentially lyophilizing, exhibited good emitted dose performance of 74.90–78.46% and FPF of 8.76–12.57% (Table V).
2. Spray-dried particles from the nozzle mixing: The aerodynamic particle size of the isoxyl microparticles produced in condition 8 was determined. The power had an emitted dose of 94% and a very low FPF of 5.4%. Therefore, cohesive forces of isoxyl microparticles were too high to achieve efficient deaggregation during aerosol dispersion. Addition of lactose carrier increased FPF of the isoxyl particles to 8.4% (Table VI).

### DISCUSSION AND FUTURE STUDIES

The commercial isoxyl consisted of either large fiber agglomerates or long fibers several hundred micrometers in length. Although the sizes of these fibers exceed the respiratory range, they can still be delivered to the lungs, due to their unique aerodynamic properties, as indicated by FPF of 6.9%. The main reason is that aerodynamic diameters of the fibers are predominantly a function of their cross-section area diameter or diameter of the small-

est dimension. Despite relatively high delivery efficiency, these fibers are not suitable for inhalation therapy: It has been well established that toxicity of certain fibers depends on particle dimension and biopersistence instead of chemical properties. It was reported that occurrence of pleural sarcoma was high in rats when the fibers were more than 4 μm long (32). One mechanism of fiber carcinogenesis is due to cell transformation. After these long fibers were phagocytized, they persist in the perinuclear region of macrophages and induce chromosomal mutations and, consequently, cell transformation (33). Also, persistence of fibers in the lungs can cause cancer and fibrosis. Macrophages cannot take up fibers much longer than their cell dimension. Phagocytosis was incomplete when the rat alveolar macrophages were exposed to fiber of 17 μm in length (34). The cut-off length of fibers causing frustrated phagocytosis by human alveolar macrophages was expected to be longer than 20 μm, because alveolar macrophages in human (diameter, ~18 μm) are larger than rats (diameter, ~13 μm) (35). Incomplete phagocytosis leads to persisting of these insoluble fibers in the lungs. As shown in “RESULTS,” commercial isoxyl particles are so long that they can be potentially persistent in the lungs and cause toxic effects. In the study, antisolvent precipitation was used to break down these long isoxyl fibers.

By simply injecting isoxyl solution into aqueous phase, the drug was precipitated out as needle-shaped particles. It was found that VRSA was a critical factor controlling particle size. Keeping other parameters consistent, isoxyl

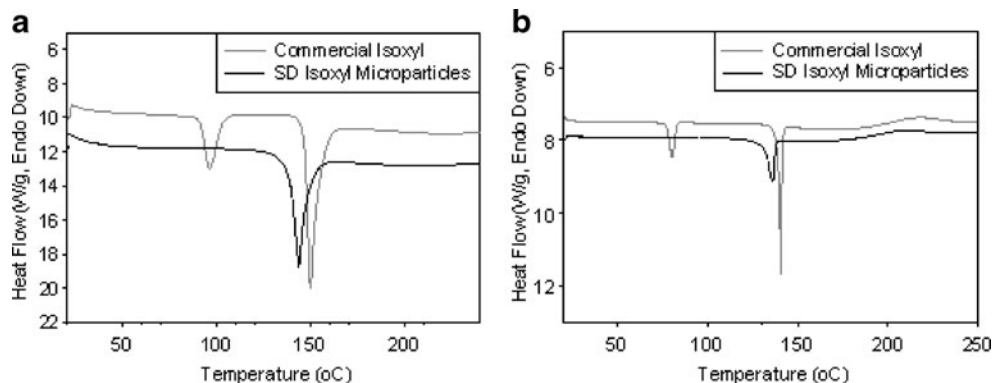


**Fig. 7.** Differential scanning calorimetry thermograms of commercial isoxyl (gray) and isoxyl microparticles (black) prepared by spray drying using condition 8. The scanning rates were 40°C/min **a** and 5°C/min **b**

**Table V.** The Deposition Profile of Each Isoxyl Powder ( $n=3$ )

	Unprocessed	VRSA=1:1	VRSA=1:2	VRSA=1:5
FPF (%)	6.94±2.34	8.76±2.61	12.57±3.35	9.23±1.65
Dispersibility (%)	8.84±3.32	10.52±4.20	16.63±3.97	12.26±2.90
Percent emission (%)	78.46±2.97	74.90±6.44	75.43±5.74	76.03±5.20
Percent recovery (%)	103.08±2.43	93.43±0.64	94.52±4.53	101.76±2.76

particle size decreased from the micron to the nano range as the VRSA were changed from 1:1 to 1:5. This is explained by increase in local supersaturation ratio ( $S$ ) and retardance in particle growth kinetics (36). Here, the local supersaturation is defined by the ratio of local drug concentration to the equilibrium solubility of drug in the mixture of solvent–antisolvent. After isoxyl ethanol solution was injected to water, solubility of the drug decreased much more in 16% ethanol (VRSA=1:5) than that in 50% ethanol (VRSA=1:1). This led to higher local supersaturation ratio in 16% ethanol and consequentially smaller nuclei. However, isoxyl nuclei were in a more dilute environment in 16% ethanol compared to 50%, which slowed down crystal growth. As a result, when VRSA was equal to 1:5, isoxyl particles were the smallest. In addition, the width of these particles was about 200 nm. This increased surface area dramatically in comparison to microsphere of the same volume, which can in turn reduce the residence time of particles in the lungs through rapid dissolution in the lung lining fluid. However, it remains to be seen whether the rapid dissolution is sufficient to achieve therapeutic isoxyl concentration systematically. If that is not true, microparticle targeting to the infected cells may be advantageous with respect to the rapid dissolution of nanoparticles and subsequent elimination of drug from the lungs before tissue penetration for therapy can occur.

The nozzle-mixing method was used to achieve uniform mixing that was hard to obtain by the manual injection method. The appropriate solvent was screened when adopting a VRSA of 1:5. Four organic solvents, ethanol, isopropanol, acetone, and THF, were selected due to their low toxicity in trace quantities. As expected, physicochemical properties of solvents were key factors controlling particle size and crystal habit. One explanation for this observation is the difference between these solvents in degree of miscibility with water, a function of supersaturation. Better miscibility resulted in higher supersaturation and smaller particle size. Also, it has been reported that an increase in supersaturation tends to form elongated particles (37). This may explain the greater production of elongated particles from ethanol or acetone than isopropanol or THF, because isopropanol is

more hydrophobic than ethanol, and acetone is completely miscible with water but THF is not. However, the effect of solvent can be complicated by other properties such as hydrogen bonding, dipole moment, and dielectric constant, which facilitate crystal growth predominately in one dimension (29). Isopropanol delivered the best product: oblate spherical nanoparticles <500 nm in length with the most homogeneous distribution.

The precipitating particles can be simultaneously spray dried. The initial aim was to collect the precipitating nanoparticle in the form of aggregates. The preparation of isoxyl particles in the study consisted of two processes: antisolvent precipitation and simultaneous spray drying, which were controlled by seven main factors: type of solvent, organic feed rate, water feed rate, inlet temperature, drug concentration, nitrogen pressure, and flow rate. Effects of these factors on particle size were evaluated in a statistically designed experiment. However, isoxyl nanoparticle aggregates could not be obtained by simply varying these operating conditions since nano-sized precipitates agglomerate into microparticles in the process. It appeared that primary sizes of the particles were determined by amount of isoxyl in the atomized droplets independent of the precipitate size. Therefore, the median diameter of the spray-dried isoxyl particles can be predicted by Eq. 1 (38):

$$d_{\text{particle}} = d_{\text{droplet}} \sqrt[3]{\frac{C}{\rho_{\text{particles}}}} \quad (1)$$

Here  $d_{\text{particle}}$  and  $d_{\text{droplet}}$  are the spray-dried particle diameter and the atomized droplet diameter.  $C$  is the concentration of isoxyl in the mixture of solvent and antisolvent, and  $\rho_{\text{particle}}$  is density of the particle. According to the information from the manufacturer (Buchi Labortechnik AG, Flawil, Switzerland), median volume diameters of the atomized droplets should be 10.48  $\mu\text{m}$  when nitrogen flow rate is 830 L/h and 30.6  $\mu\text{m}$  when nitrogen flow rate is 440 L/h. Assuming the median volume diameter of the atomized droplets is around 20  $\mu\text{m}$  for 600 L/h and density of isoxyl is close to 1  $\mu\text{g}/\text{ml}$ , the median diameter of resulting isoxyl particles is predicted to be between 0.92 and 2.7  $\mu\text{m}$ , which is consistent with the experimental results. This also explains the production of larger microparticles when THF was used as solvent. Isoxyl has a higher solubility in THF than alcohols. Theoretically, during antisolvent precipitation process, smaller particles should precipitate due to an increasing local supersaturation. However, the result showed that final particle size of the spray-dried particles from THF was much larger than those from alcohols because a higher concentration of isoxyl was present in one atomized droplet during spray drying.

**Table VI.** The Deposition Profile of Isoxyl Microparticles in Condition 8 ( $n=3$ )

	Microparticles without lactose	Microparticles with lactose
FPF (%)	5.4±1.7	8.4±1.6
Dispersibility (%)	5.8±1.9	8.7±1.7
Percent emission (%)	94.2±2.3	96.6±0.2
Percent recovery (%)	91.1±3.1	97.4±1.8

The spray-drying method failed to produce isoxyl nanoparticle aggregates due to irreversible agglomeration which commonly occurs. The isoxyl nanoparticles can only exist as separate particles in a dilute suspension. In order to conduct *in vivo* disposition and efficacy studies, this diluted nanoparticle suspension can be made immediately prior to delivery by nebulizer. The spray-dried nanoparticle aggregates may be prepared by using appropriate surfactants and/or bulking agents. Theoretically, appropriate stabilizers can slow growth of the particles by condensation and coagulation, which reduces particle sizes. Stabilizers and bulking agents can also cover the precipitating particles and prevent them from agglomerating in the drying process and during a long-term storage. The bulking agent, mannitol, was evaluated in the study. Nanoparticle aggregates were produced, but these particles were heterodisperse. Therefore, either mannitol itself or the amount of mannitol was not sufficient to prevent nanoparticle agglomeration. Further studies are needed to screen suitable surfactants or bulking agents for isoxyl nanoparticle preparation. The choice of surfactants is very limited for pulmonary delivery. Sodium oleate, sodium stearate, cetyl alcohol, tyloxapol, pluronics, lactose, mannitol, polyvinyl alcohol, polyethylene glycol, and hydroxypropylmethylcellulose may be considered, although not all of these are present in approved products. Some of them are present in Food and Drug Administration-approved inhalation products, while some of them have been studied extensively and are generally recognized as safe. Theoretically, 30–40% *w/w* of these stabilizing agents is required to keep nanoparticles with diameters between 120 and 300 nm separate (39).

The crystalline/amorphous states influence many physicochemical properties of drugs such as saturation solubility, moisture sorption, and particle stability (40,41). Isoxyl is known to exist in two different crystal forms. The needle crystals by crystallization from ethanol have higher melting point of 149°C ( $\Delta H=98$  J/g) and lower aqueous solubility of 0.88  $\mu\text{g/ml}$  than these from hexane that have melting point of 141°C ( $\Delta H=77$  J/g) and aqueous solubility of 17.8  $\mu\text{g/ml}$  (42). During synthesis, isoxyl was purified by crystallization of the drug from ethanol (43). As expected, DSC profiles showed that the commercial isoxyl powder contains crystal form I and a large quantity of residual ethanol. In comparison, micro-particle processing improved properties of isoxyl in the following ways: (1) Spray drying completely removed the residual ethanol; (2) conversion of isoxyl crystal form I to form II occurred. These phenomena contributed to expectations of much higher solubility. However, it remains to be established whether polymorph conversion occurred during precipitation from isopropanol/water or spray drying.

The needle-shaped isoxyl particles generated from the injection method and lyophilization exhibited higher FPF and lower emitted dose than those spherical particles from the nozzle mixing and spray drying. Theoretically, particle shape greatly impacts on their dispersion and aerodynamic behavior (44,45). Inspiratory flow fluidizes and deaggregates particles delivered for the Inhalator®, a passive dry powder inhaler. Dispersion of particles composes several processes: dilation, flow, fluidization, and deaggregation. The interparticulate interaction between elongated particles is very unstable. After the elongated particles are dispersed, most of them line up along air streams. As a result, their aerodynamic

diameters only depend on their shortest dimension and independent of their length. When these particles are inhaled to the respiratory tract, they will travel further and achieve better deposition in the deep lung than the spherical particles with the same geometric diameters (31,44–47). Consequently, the elongated particles achieved high FPF due to apparently good dispersion and aerodynamic properties. However, the flow property of needle-shaped particles is worse than spherical particle. This caused more particles to adhere to the wall of capsule inside the device and resulted in lower emitted dose. The spray-dried isoxyl microparticles were delivered following blending with carrier lactose, which increased FPF from 5.4% to 8.4%. Further work is required to improve the performance of lactose blends with isoxyl.

## CONCLUSION

Antisolvent precipitation in water was used to prepare isoxyl particles suitable for lung delivery. Nanoparticles with a count median width of 275 nm and a count median length of 495 nm were produced using isopropanol as a solvent and a VRSA equal to 1:5. Spray drying failed to collect these nanoparticles but generated near spherical microparticles with a count median diameter of 1–2  $\mu\text{m}$ . Addition of mannitol in antisolvent at a drug to mannitol ration of 1:4.4 during processing produced isoxyl nanoparticle aggregates. A range of microparticle and nanoparticle preparations has been evaluated. Further work on their delivery as aerosols is required to assess the potential for inhaled treatment of tuberculosis.

## ACKNOWLEDGEMENTS

Scanning electron microscopy was conducted at the Analytical and Nanofabrication Laboratory (CHANL) and the School of Dentistry, University of North Carolina at Chapel Hill. We gratefully acknowledge the assistance of Carrie Donley and Wallace Ambrose.

## REFERENCES

1. WHO. World Health Organization report: global tuberculosis control—epidemiology, strategy, financing. Geneva: WHO; 2009.
2. Frieden TR, Sterling TR, Munsiff SS, Watt CJ, Dye C. Tuberculosis. *Lancet*. 2003;362(9387):887–99.
3. Gelperina S, Kisich K, Iseman MD, Heifets L. The potential advantages of nanoparticle drug delivery systems in chemotherapy of tuberculosis. *Am J Respir Crit Care Med*. 2005;172(12):1487–90.
4. Bastian I, Colebunders R. Treatment and prevention of multi-drug-resistant tuberculosis. *Drugs*. 1999;58(4):633–61.
5. Skeiky YA, Sadoff JC. Advances in tuberculosis vaccine strategies. *Nat Rev Microbiol*. 2006;4(6):469–76.
6. Kimerling ME, Phillips P, Patterson P, Hall M, Robinson CA, Dunlap NE. Low serum antimycobacterial drug levels in non-HIV-infected tuberculosis patients. *Chest*. 1998;113(5):1178–83.
7. Conte Jr JE, Golden JA, McQuitty M, Kipps J, Duncan S, McKenna E *et al*. Effects of gender, AIDS, and acetylator status on intrapulmonary concentrations of isoniazid. *Antimicrob Agents Chemother*. 2002;46(8):2358–64.
8. Tappero JW, Bradford WZ, Agerton TB, Hopewell P, Reingold AL, Lockman S *et al*. Serum concentrations of antimycobacterial drugs in patients with pulmonary tuberculosis in Botswana. *Clin Infect Dis*. 2005;41(4):461–9.
9. Muttill P, Wang C, Hickey AJ. Inhaled drug delivery for tuberculosis therapy. *Pharm Res*. 2009;26:2401–16.

10. Hwang SM, Kim DD, Chung SJ, Shim CK. Delivery of ofloxacin to the lung and alveolar macrophages via hyaluronan microspheres for the treatment of tuberculosis. *J Control Release*. 2008;129(2):100–6.
11. Davies NM, Feddah MR. A novel method for assessing dissolution of aerosol inhaler products. *Int J Pharm*. 2003;255(1–2):175–87.
12. Patton JS, Fishburn CS, Weers JG. The lungs as a portal of entry for systemic drug delivery. *Proc Am Thorac Soc*. 2004;1(4):338–44.
13. Makino K, Nakajima T, Shikamura M, Ito F, Ando S, Kochi C *et al*. Efficient intracellular delivery of rifampicin to alveolar macrophages using rifampicin-loaded PLGA microspheres: effects of molecular weight and composition of PLGA on release of rifampicin. *Colloids Surf B Biointerfaces*. 2004;36(1):35–42.
14. Phetsuksiri B, Baulard AR, Cooper AM, Minnikin DE, Douglas JD, Besra GS *et al*. Antimycobacterial activities of isoxyl and new derivatives through the inhibition of mycolic acid synthesis. *Antimicrob Agents Chemother*. 1999;43(5):1042–51.
15. Isoxyl. *Tubercle*. 1965;46(3):298–300.
16. Tousek J. On the clinical effectiveness of isoxyl. *Antibiot Chemother*. 1970;16:149–55.
17. Bartmann K, editor. *Antituberculosis drugs*. Berlin: Springer-Verlag; 1988. p. 185–9.
18. Mitchell RS, Petty TL, Dye WE. Clinical and pharmacological studies of isoxyl. In *Transactions of the 23rd Research Conference in Pulmonary Disease*; 1964.
19. Wang Z, Chen JF, Le Y, Shen ZG, Yun J. Preparation of ultrafine beclomethasone dipropionate drug powder by antisolvent precipitation. *Ind Eng Chem Res*. 2007;46(14):4839–45.
20. Patton JS, Byron PR. Inhaling medicines: delivering drugs to the body through the lungs. *Nat Rev Drug Discov*. 2007;6(1):67–74.
21. Tam JM, McConville JT, Williams 3rd RO, Johnston KP. Amorphous cyclosporin nanodispersions for enhanced pulmonary deposition and dissolution. *J Pharm Sci*. 2008;97:4915–33.
22. Ahsan F, Rivas IP, Khan MA, Torres Suarez AI. Targeting to macrophages: role of physicochemical properties of particulate carriers–liposomes and microspheres–on the phagocytosis by macrophages. *J Control Release*. 2002;79(1–3):29–40.
23. Sharma R, Saxena D, Dwivedi AK, Misra A. Inhalable microparticles containing drug combinations to target alveolar macrophages for treatment of pulmonary tuberculosis. *Pharm Res*. 2001;18(10):1405–10.
24. Sharma R, Muttill P, Yadav AB, Rath SK, Bajpai VK, Mani U *et al*. Uptake of inhalable microparticles affects defence responses of macrophages infected with *Mycobacterium tuberculosis* H37Ra. *J Antimicrob Chemother*. 2007;59(3):499–506.
25. Tam JM, McConville JT, Williams 3rd RO, Johnston KP. Amorphous cyclosporin nanodispersions for enhanced pulmonary deposition and dissolution. *J Pharm Sci*. 2008;97(11):4915–33.
26. Matteucci ME, Hotze MA, Johnston KP, Williams 3rd RO. Drug nanoparticles by antisolvent precipitation: mixing energy *versus* surfactant stabilization. *Langmuir*. 2006;22(21):8951–9.
27. Mullin JW. *Crystallization*. 4th ed. Oxford: Butterworth-Heinemann; 2001.
28. Adamson AW. *Physical chemistry of surfaces*. 5th ed. New York: Wiley; 1990.
29. Park SJ, Yeo SD. Antisolvent crystallization of sulfa drugs and the effect of process parameters. *Sep Sci Technol*. 2007;42:2645–60.
30. Cal K, Sollohub K. Spray drying technique. I: Hardware and process parameters. *J Pharm Sci*. 2010;99:575–86.
31. Larhrib H, Martin GP, Marriott C, Prime D. The influence of carrier and drug morphology on drug delivery from dry powder formulations. *Int J Pharm*. 2003;257(1–2):283–96.
32. Stanton MF, Layard M, Tegeris A, Miller E, May M, Morgan E *et al*. Relation of particle dimension to carcinogenicity in amphibole asbestoses and other fibrous minerals. *J Natl Cancer Inst*. 1981;67(5):965–75.
33. Barrett JC, Lamb PW, Wiseman RW. Multiple mechanisms for the carcinogenic effects of asbestos and other mineral fibers. *Environ Health Perspect*. 1989;81:81–9.
34. Blake T, Castranova V, Schwegler-Berry D, Baron P, Deye GJ, Li C *et al*. Effect of fiber length on glass microfiber cytotoxicity. *J Toxicol Environ Health A*. 1998;54(4):243–59.
35. Zeidler-Erdely PC, Calhoun WJ, Ameredes BT, Clark MP, Deye GJ, Baron P *et al*. *In vitro* cytotoxicity of Manville Code 100 glass fibers: effect of fiber length on human alveolar macrophages. *Part Fibre Toxicol*. 2006;3:5.
36. Zhao H, Le Y, Liu H, Hu T, Shen Z, Yun J *et al*. Preparation of microsized spherical aggregates of ultrafine ciprofloxacin particles for dry powder inhalation (DPI). *Powder Technol*. 2009;194:81–6.
37. Haleblan JK. Characterization of habits and crystalline modification of solids and their pharmaceutical applications. *J Pharm Sci*. 1975;64(8):1269–88.
38. Vehring R. Pharmaceutical particle engineering via spray drying. *Pharm Res*. 2008;25(5):999–1022.
39. Chow AH, Tong HH, Chattopadhyay P, Shekunov BY. Particle engineering for pulmonary drug delivery. *Pharm Res*. 2007;24(3):411–37.
40. Muller RH, Jacobs C, Kayser O. Nanosuspensions as particulate drug formulations in therapy. Rationale for development and what we can expect for the future. *Adv Drug Deliv Rev*. 2001;47(1):3–19.
41. Hickey AJ. *Inhalation aerosols: physical and biological basis for therapy*. 2nd ed. New York: Informa Healthcare; 2006.
42. Caira M, Crider M, de Villers M, Liebenberg W. New synthesis and physicochemical properties of two crystal forms of the antitubercular agent isoxyl. In: *AAPS Annual Meeting and Exposition*; 2005.
43. Bhowruth V, Brown AK, Reynolds RC, Coxon GD, Mackay SP, Minnikin DE *et al*. Symmetrical and unsymmetrical analogues of isoxyl; active agents against *Mycobacterium tuberculosis*. *Bioorg Med Chem Lett*. 2006;16(18):4743–7.
44. Hinds WC. *Aerosol technology: properties, behavior, and measurement of airborne particles*. 2nd ed. New York: Wiley; 1998.
45. Dunbar CA, Hickey AJ, Holzner P. Dispersion and characterization of pharmaceutical dry powder aerosols. *KONA*. 1998;16:7–44.
46. Hickey AJ. *Pharmaceutical inhalation aerosol technology*, vol. 2. New York: Marcel Dekker Inc; 2003 (revised and expanded).
47. Zeng XM, Martin AP, Marriott C, Pritchard J. The influence of carrier morphology on drug delivery by dry powder inhalers. *Int J Pharm*. 2000;200(1):93–106.